



HAL
open science

CMT-based wire arc additive manufacturing of Inconel 625 alloy

Ji Junwen, Anatoliy Zavdoveev, Dmytro Vedel, Thierry Baudin, Sviatoslav Motrunich, Ilya Klochkov, Sabine Friederichs, Natalia Strelenko, Mykola Skoryk

► **To cite this version:**

Ji Junwen, Anatoliy Zavdoveev, Dmytro Vedel, Thierry Baudin, Sviatoslav Motrunich, et al. CMT-based wire arc additive manufacturing of Inconel 625 alloy. *Emerging Materials Research*, 2023, 12 (3), pp.315-322. <10.1680/jemmr.23.00053>. <hal-04245365>

HAL Id: hal-04245365

<https://hal.science/hal-04245365v1>

Submitted on 17 Oct 2023

HAL is a multi-disciplinary open access archive for the deposit and dissemination of scientific research documents, whether they are published or not. The documents may come from teaching and research institutions in France or abroad, or from public or private research centers.

L'archive ouverte pluridisciplinaire **HAL**, est destinée au dépôt et à la diffusion de documents scientifiques de niveau recherche, publiés ou non, émanant des établissements d'enseignement et de recherche français ou étrangers, des laboratoires publics ou privés.



HAL Authorization

CMT-based wire arc additive manufacturing of Inconel 625 alloy

J. Junwen¹, A. Zavdoveev², D. Vedel³, T. Baudin⁴, S. Motrunich^{2x}, I. Klochkov^{2x}, S. Friederichs⁵,
N. Strelenko¹, M. Skoryk^{6x}

¹ National Technical University of Ukraine "Igor Sikorsky Kyiv Polytechnic Institute", 37, Prosp. Peremohy, Kyiv, Ukraine

² Paton Electric Welding Institute of NAS of Ukraine, K. Malevicha n. 11, 03680 Kiev, Ukraine, avzavdoveev@gmail.com

³ I. M. Frantsevich Institute of Problems of Materials Science NAS of Ukraine, st. Krzyzanowski, 303142, Kyiv, Ukraine, e-mail: vedeldv@gmail.com

⁴ Université Paris-Saclay, CNRS, Institut de chimie moléculaire et des matériaux d'Orsay, 91405 Orsay, France, thierry.baudin@universite-paris-saclay.fr

⁵ Clausthal University of Technology, 1775, Clausthal-Zellerfeld, Germany

⁶ G. V. Kurdyumov Institute of Metal Physics of the NAS of Ukraine; Kyiv, Ukraine, e-mail: mykolaskor@gmail.com

Abstract:

Cold metal transfer (CMT) technology is considered in an application for wire arc additive manufacturing WAAM of refractory high corrosion resistant Inconel 625 alloy. Based on the fabricated wall it has been shown the suitability of CMT WAAM for the sound formation of weld and homogenous distribution of mechanical properties. Microscopy analysis has revealed that the microstructure of the deposited alloy along the height of the wall element is quite uniform. The minor differences in the microstructure are observed in the bottom part, caused by welding specifically.

Key words: cold metal transfer, wire arc additive manufacturing, Inconel 235, structure, mechanical properties

Abbreviations

AM – additive manufacturing

BSE – backscattered electrons

E – Young's modulus

EDX – energy dispersive X-Ray analysis

GMAW – gas metal arc welding

HV – Vickers hardness

SE – secondary electrons

SEM – scanning electron microscopy

UTS – ultimate tensile stress

WAAM – wire arc additive manufacturing

WTC – welding thermal cycle

YS – yield stress

Introduction

Inconel 625 is a high-performance nickel-chromium-molybdenum alloy with a higher nickel content than other grades of Inconel. It has a high melting point, strength, and resistance to high temperatures. In addition, it has good anti-corrosion and anti-oxidation properties [1,2]. These properties make it frequently used in nuclear reactors, aviation, and marine engineering [3,4]. The shapes of most of the Inconel 625 components are so complex that they are expensive to produce using traditional methods due to extensive machining [5,6]. The researchers concluded that the CMT-WAAM technique is better than the cast Inconel 625 parts based on mechanical properties [7–10]. The fabrication of aircraft landing gear ribs through WAAM technology is the recent breakthrough in WAAM technology with savings of 78 % of raw material cost compared to other traditional subtractive machining processes [5,11,12].

Wire Arc Additive Manufacturing (WAAM) using arc as a heat source has simple forming equipment, low equipment cost, high material utilization rate and deposition efficiency of forming process, and is suitable for rapid prototyping of large-sized components. Compared with traditional subtractive manufacturing, arc additive manufacturing can shorten the forming time by 40% to 60%, the material utilization rate is high, and the subsequent machining time can also be shortened by 15% to 20% [13,14]. Cold metal transfer (CMT) arc additive manufacturing technology has the advantages of low heat input, high deposition efficiency, and stable forming, and has broad application prospects in the field of direct forming of large-scale components [15,16].

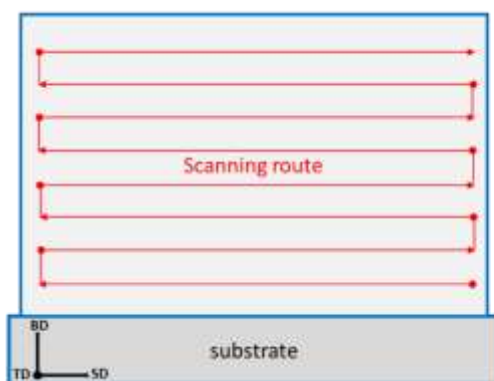
This paper studies the use of cold metal transfer (CMT) technology using nickel-based alloy 625 as the welding wire with accents on mechanical properties and microstructure of manufactured wall element.

Experimental.

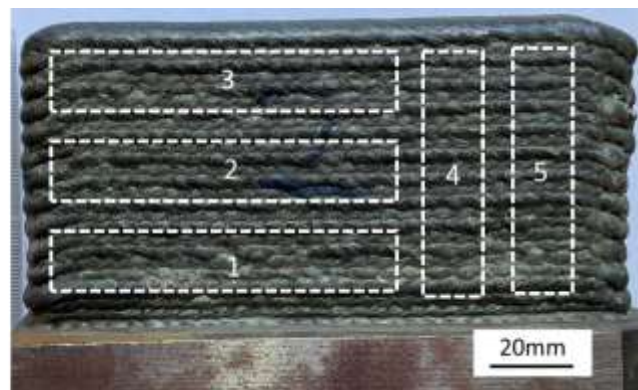
The cold metal transfer technology based on Fronius TPS 5000 power supply was used as a direct energy deposition method. Filler material INCONEL Filler Metal 625 (UNS N06625, ISO 15156-3) was used for arc welding in an environment of protective gases with a diameter of 1.2 mm used for the WAAM. The metal deposition procedure was realized with the robotic arm ABB2600. The deposition welding mode was taken as optimal according to Fronius's specification for the particular welding consumables and is presented in Table 1. For the substrate were chose as rolled low-carbon steel plate with a 20mm thickness. The scanning route and fabricated wall element are schematically shown in fig.1a. Highlighted samples (fig.1 b) were further investigated for mechanical properties characterization (numbers 1-4) and metallography (number 5).

Table 1. CMT welding mode.

Consumable	Welding speed, mm/s	Wire feed, m/min	Shield gas	Gas flow, l/min	Welding current, A	Welding voltage, V	Number of layers	Interlayer temperature, °C
INCONEL Filler Metal 625	10	4.3	Ar, 99,99%	15	107	15.9	25	100



(a)



(b)

Figure 1. Schematic illustration of the deposition route (a) and final fabricated wall element (b); BD-building direction, SD-scanning direction, TD-transverse direction.

The mechanical properties of samples 1-4 cut from wall element, i.e., ultimate tensile strength (UTS), yield stress (YS) and plasticity (δ - uniform elongation for failure), were determined in static tensile tests at ambient temperature. The cylindrical samples with a 6mm diameter of the working part were machined. The tensile test was utilized on the universal servohydraulic complex MTS 318.25 with a maximum force of 250 kN. To establish the effect of the chosen technology on material strength Vickers hardness tests were performed with loads of 100 g for 10 s, 3 measurements per point.

For structural analysis, several methods were used: scanning electron microscopy (SEM, with a Tscan Mira 3 LMU facility), and energy dispersive spectroscopy (EDS from Oxford Instruments). The preparation of metallographic specimens for microstructural studies was carried out according to standard methods using grinding papers of various roughnesses (P240, P400, P600, P1200, P2000). Final polishing was performed on a diamond suspension with a polishing particle size of 1 μm . To reveal and identify the morphology of the microstructure of the specimen, electrochemical etching with chromic anhydride 14% water solution was used. Etching parameters were as follows anodic current density, 1 A/cm^2 , voltage 23 V, and exposure time 19 s, with consequent washing and drying.

Results and discussion

To characterize the properties of the wall element of the Inconel 625 alloy made by electric arc welding using cold metal transfer technology, a set of studies was performed, such as Vickers hardness measurement, determination of strength and plasticity indicators, as well as microstructure analysis.

Mechanical properties characterization

The hardness measurement was carried out on specimens that were cut from the bottom, middle and top part of the printed wall (BD-TD plane). The graph presents the measurement results along with the layout in figure 2a. The average hardness of the specimen was: 269 ± 19 HV bottom, 260 ± 17 HV middle, and 267 ± 42 HV top. These results show no explicit average hardness value varies between different parts of the deposited metal. The scatter of the hardness values along the (vertical) built direction corresponds with the microstructure features formed during manufacturing. Firstly, this is conditioned by the welding process peculiarity, namely previous layers are subjected to reheating during the subsequent layer deposition.

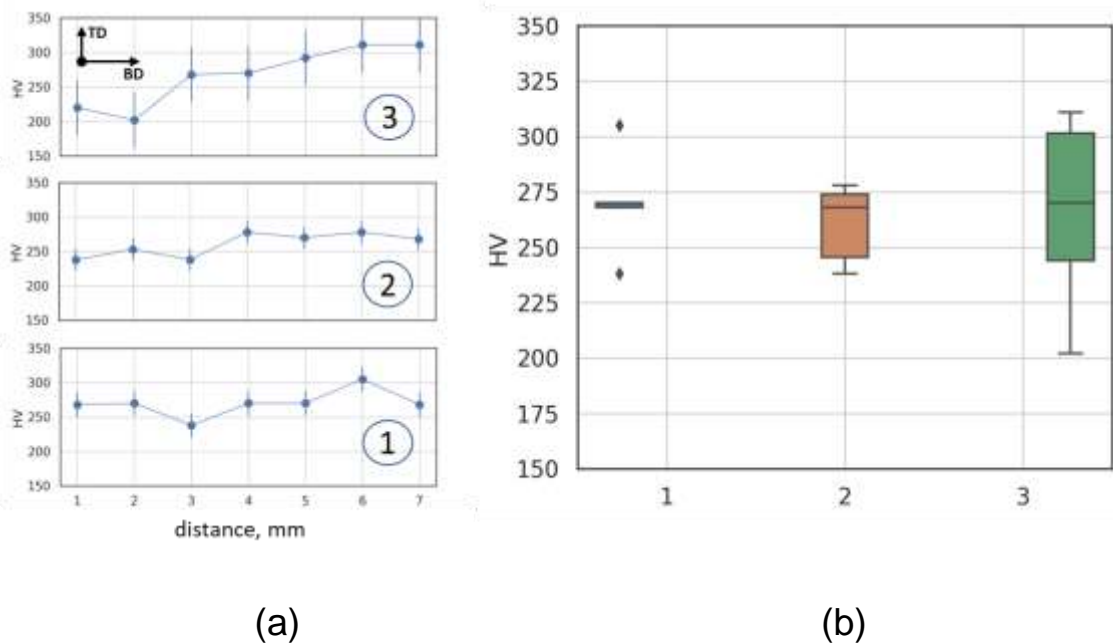


Figure 2. Vickers hardness distribution at the bottom (1), middle (2), and top (3) part of the wall element, linear distribution(a), average value boxplot (b)

The results of tensile tests at ambient temperature are shown in table 2 and figure 3. The standard deviations of yield stress and ultimate tensile

stress do not exceed 2% and 3%, respectively. The uniform distribution of the elongation values is observed for all (1-4) tested samples, which evidences the homogenous structure of the samples. The UTS values in the horizontal direction for CMT WAAM are slightly higher than those in the cross direction, while there is no explicit variation observed in YS values. The YS for the studied areas are 383 MPa, 384 MPa, and 370 MPa, respectively. During tests in the transverse direction, the strength indicators decrease by 4% to 371MPa, which is caused by the anisotropy of the structure and the formation of the welded rollers. From the given data, it is clearly visible that the mechanical properties are uniform over the entire height of the wall element. At the same time, there is a tendency for a slight decrease in strength indicators in the upper layers of the surfacing, but within a 5% margin of error.

Table 2. Mechanical properties of the CMT WAAMed Inconel 625 wall element

	YS, MPa	UTS, MPa	δ_5 , %	ψ , %
bottom	383,1	712,1	27%	56%
middle	384,5	688,6	26%	59%
top	370,5	671,4	25%	53%
cross	371,9	661,5	28%	76%

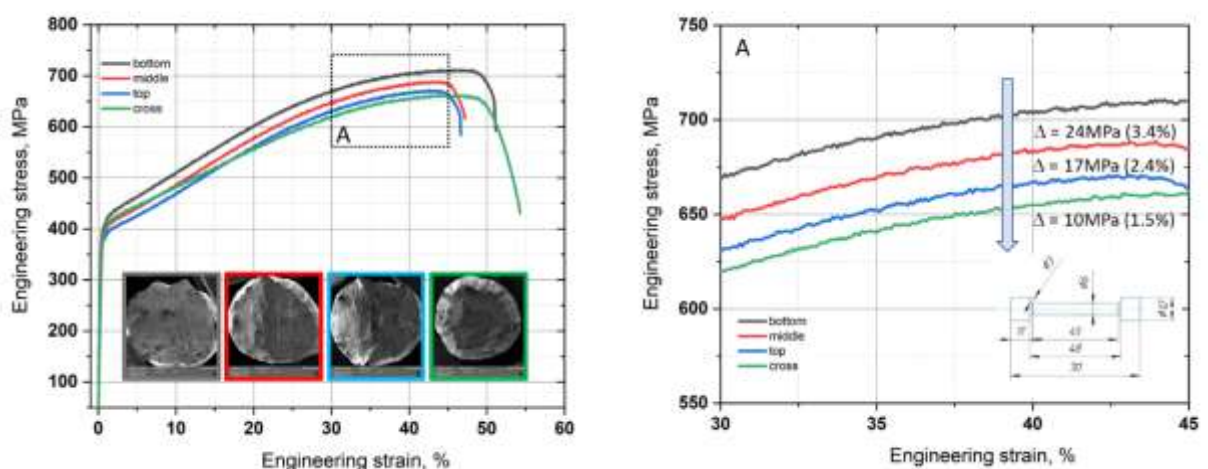


Figure 3. Engineering stress-strain curves for CMT WAAMed Inconel 625 wall element

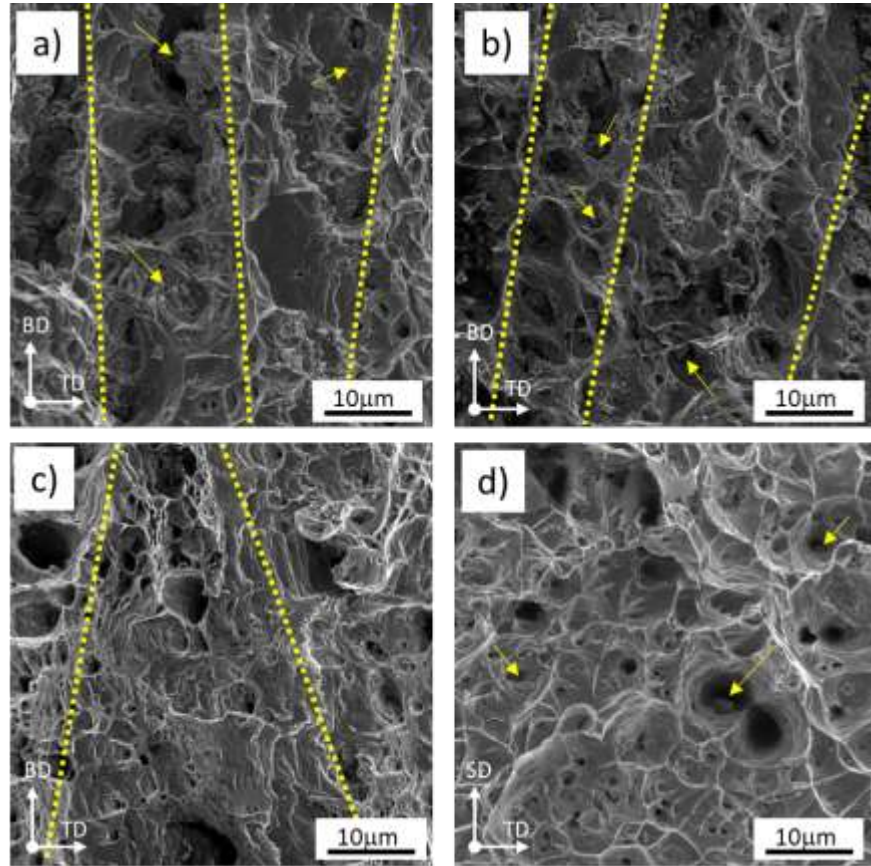


Figure 4. The fracture surface of the CMT WAAMed Inconel 625 wall element samples: bottom (a), middle (b), top (c) cross (d).

This behavior of mechanical properties is determined by the peculiarities of structure formation during multilayer surfacing and will be considered below.

The corresponding fractograms for tensiled samples are presented in figure 4. With yellow dotted lines, the dendritic arms' positions are highlighted. The overall character of the fracture is ductile with mixed morphology for horizontal samples (fig. 4 a - c), namely the simultaneous existence of zones with small size dimples as well as big ones preferably allocated interdendritically. The vertical (cross) sample (fig. 4 d) has different morphology, with no explicit traces of dendritic structure, and the dimples are uniform and distributed homogeneously. This is the course of an increased level of plasticity in the vertical (cross) direction of the wall

element. Such character of fracture surfaces is in strong agreement with mechanical test data.

Microstructure characterization

Inconel 625 is a nickel-based superalloy that is known for its excellent corrosion resistance, high strength, and good weldability. Its microstructure comprises a face-centered cubic (FCC) crystal structure with a matrix of nickel-chromium-molybdenum alloying elements. The microstructure of Inconel 625 can be further described as a two-phase structure consisting of a solid solution matrix and a dispersion of finely dispersed coherent particles of the intermetallic compound Ni_3Nb . The solid solution matrix is composed mainly of nickel and chromium, with smaller amounts of molybdenum, iron, and other elements, such as niobium, carbon, and silicon, depending on the specific composition. The presence of niobium in the alloy helps to stabilize the matrix and improve its strength and resistance to deformation, while the dispersion of Ni_3Nb particles provides additional strengthening and improves resistance to creep and fatigue.

The micrographs (Figure 5) obtained from etched specimens revealed the distinct layers that are typical of additive manufacturing technologies along with the boundaries of the molten pool. The microstructure displays a dendritic pattern oriented in the same direction, with a relatively fine grained at the layer boundaries. Although not cellular, the microstructure is akin to that of welded microstructure.

The as-welded microstructure consists of columnar dendrites, as depicted in Figure 5. There is a tendency to crush dendritic branches at the transition points on the fused lines between successive layers. In addition, when approaching the upper part of the wall element, the dendritic branches become more elongated and branched. This is due to the fact that the previous layers underwent repeated thermal exposure during the multilayer deposition and the metal was subjected to welding tempering,

which probably induced additional dispersion strengthening and structure modification. At the same time, the upper layers of the surfacing have a characteristic/close to as cast structure [12,17,18].

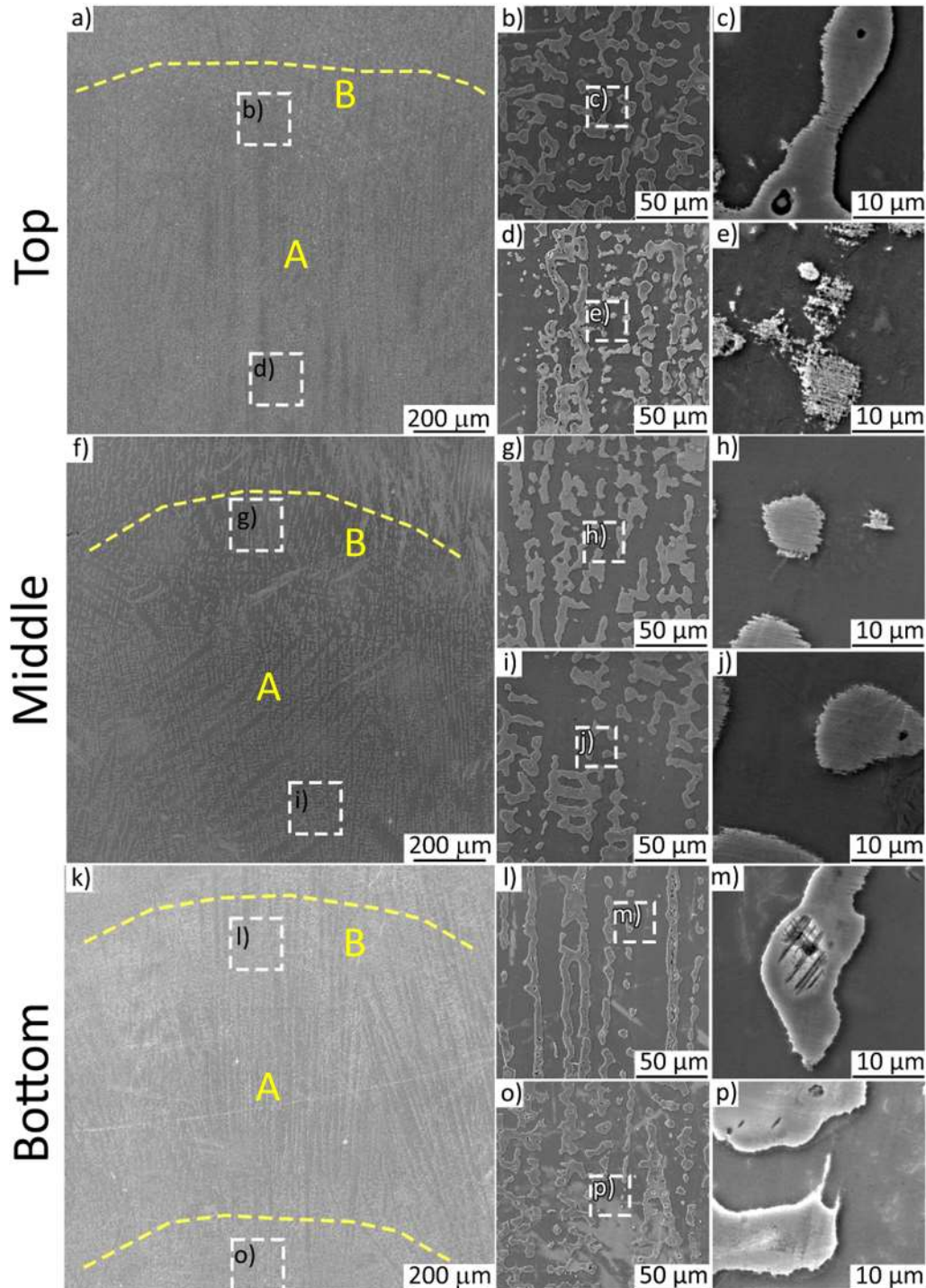
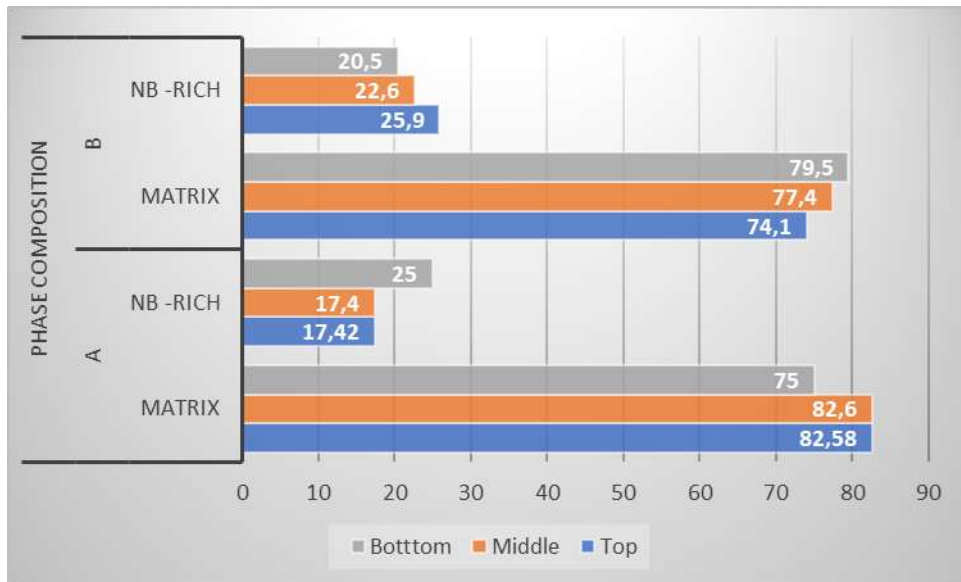
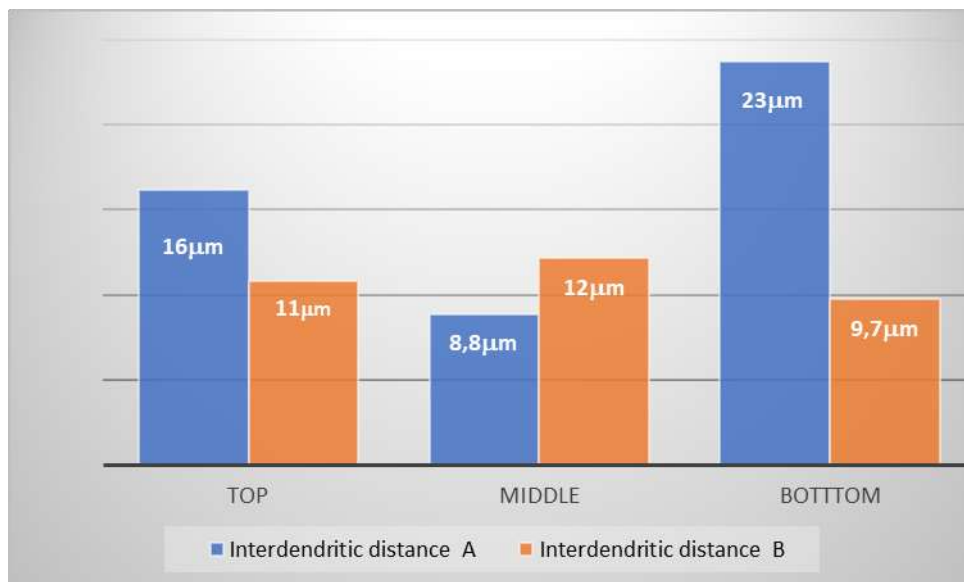


Figure 5. SEM microstructure of the CMT WAAMed Inconel 625 wall element (BD-TD plane). (a-e) – Top, (f-j) – Middle (k-p) – Bottom zones of the billet. 'A' indicate middle zone of layer, 'B' - layers interface.



a)



b)

Figure 6. Quantitative data for microstructure (figure 5): phase composition (a), dendritic arms size (b). 'A' indicate middle zone of layer, 'B' - layers interface.

Two types of cellular-dendritic microstructures were observed in the as-welded. Two kinds of microstructures exhibit similar growth directions and appear alternatively (Figure 5). The arm spacing of the continuous cellular-dendritic microstructure ranges from 8-23 μm (Figures 5 and 6b). Quantitative analysis has shown some differences at the interface and middle part of layers (figure 6 b.). Namely, the matrix and Nb rich phase

ratio slightly differs which is a natural phenomenon for multilayer deposition (Figure 6a). This effect is caused by thermal gradient during consequent deposition on 100 °C preheated previous layer [19]. This solidification condition differs from the interface to the top part of the layer. The overall microstructure distribution at different scales can be counted as uniform.

Light and dark zones are distinguished in figure 5?, the first of which are the axes of dendrites, and the second interdendritic zones are depleted in the content of Nb chemical element (Fig. 7). This effect is explained by the peculiarities of the crystallization of the molten metal and liquation during the hardening of the metal. Light zones are enriched with niobium, while dark zones are depleted.

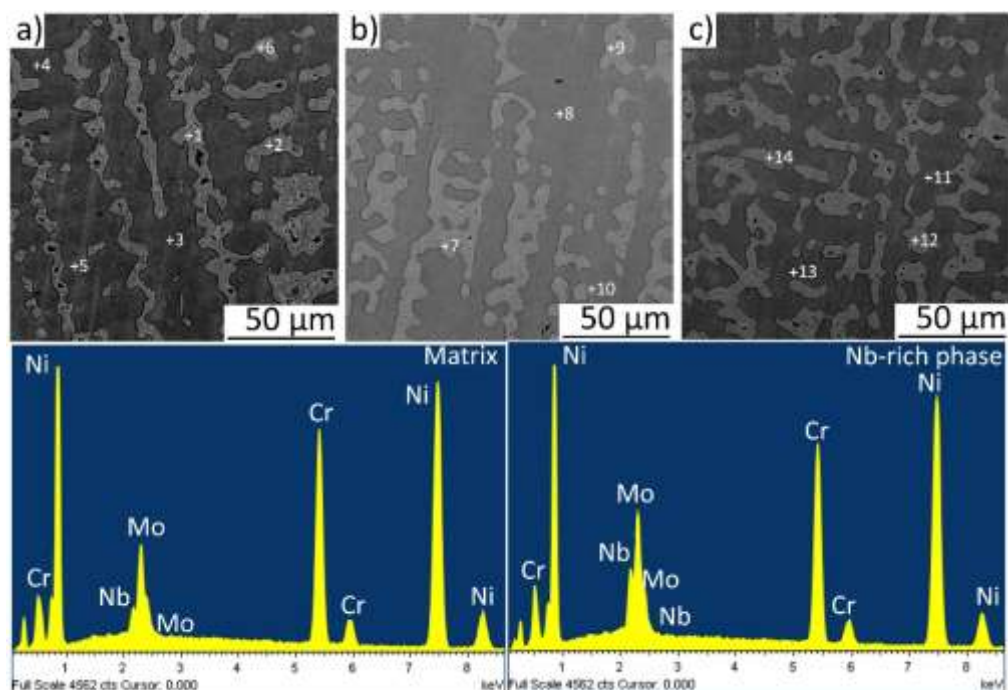


Figure 7. Composition peculiarities of the dendritic structure at the bottom (a) middle (b) and top (c) zones of CMT WAAMed Inconel 625 wall element

At the bottom part of the printed sample, the alloy matrix is depleted with Nb (figure 6a, table 3), possibly due to solidification conditions as the first deposition is conducted on a cold substrate. And further subjected to multiple thermal cycles of welding. The middle and top parts have similar

chemical elements distribution as well as in the matrix and Nb-rich phase. Such an effect is closely connected with the similar condition of steady state manufacturing mode (preheating of the previous layer, solidification).

Table 3. Main alloying element distribution for matrix and Nb-rich phase CMT WAAMed Inconel 625 wall element

	Cr	Ni	Nb	Mo
bottom				
Nb rich phase	21.36	56.59	8.93	13.11
Matrix	23.34	63.80	2.57	10.30
Macro	23.07	61.38	4.43	11.12
middle				
Nb rich phase	22.60	59.26	5.84	12.30
Matrix	23.38	63.47	2.90	10.24
Macro	23.12	61.14	4.63	11.11
top				
Nb rich phase	21.62	58.25	7.72	12.41
Matrix	23.26	62.42	3.47	10.85
Macro	23.14	60.91	4.54	11.41

The macro analysis of chemical composition at the bottom, middle, and top parts has shown good uniformity of main alloying element distribution (table 3).

Conclusions

The objective of this investigation was to examine the material characteristics of a CMT WAAM technique utilized for Inconel 625 material. The outcomes of this WAAM method indicated the applicability of CMT, owing to its reduced heat input, as a direct energy deposition power source. The material analysis indicated that the CMT WAAM method provides advantages in terms of the mechanical properties and microstructure homogeneity of produced components.

Acknowledgments

Ji Junwen is acknowledged for Scholarship from the Chinese Scholarships Council and for Ukrainian academic scholarship for outstanding results. The authors are grateful Dr. A. Shishkevich (PWI NAS of Ukraine) for the help in experiments.

Conflict of interest: Ji Junwen, Anatoliy Zavdoveev, Dmytro Vedel, Thierry Baudin, Sviatoslav Motrunich, Ilya Klochkov, Sabine Friederichs, Natalia Strelenko, Mykola Skoryk declare that they have no conflict of interest.

Author Contributions: Anatoliy Zavdoveev, Conceptualization, Methodology
Anatoliy Zavdoveev, Thierry Baudin Supervision Ji Junwen, Dmytro Vedel,
Sviatoslav Motrunich, Ilya Klochkov, Sabine Friederichs, Natalia Strelenko and
Mykola Skoryk Data curation, Writing- Original draft preparation. All authors discussed the results and commented on the manuscript.

Reference

- [1] V. Shankar, K.B.S. Rao, S.L. Mannan, Microstructure and mechanical properties of Inconel 625 superalloy, *J. Nucl. Mater.* 288 (2001) 222–232.
- [2] D. Li, Q. Guo, S. Guo, H. Peng, Z. Wu, The microstructure evolution and nucleation mechanisms of dynamic recrystallization in hot-deformed Inconel 625 superalloy, *Mater. Des.* 32 (2011) 696–705.
- [3] S.S. Sandhu, A.S. Shahi, Metallurgical, wear and fatigue performance of Inconel 625 weld claddings, *J. Mater. Process. Technol.* 233 (2016) 1–8.
- [4] X. Lou, D. Gandy, Advanced manufacturing for nuclear energy, *Jom.* 71 (2019) 2834–2836.
- [5] Z. Qiu, B. Wu, H. Zhu, Z. Wang, A. Hellier, Y. Ma, H. Li, O. Muransky, D. Wexler, Microstructure and mechanical properties of wire arc additively manufactured Hastelloy C276 alloy, *Mater. Des.* 195 (2020) 109007.

- [6] M. Karmuhilan, S. Kumanan, A review on additive manufacturing processes of inconel 625, *J. Mater. Eng. Perform.* (2021) 1–10.
- [7] F. Xu, Y. Lv, Y. Liu, F. Shu, P. He, B. Xu, Microstructural evolution and mechanical properties of Inconel 625 alloy during pulsed plasma arc deposition process, *J. Mater. Sci. Technol.* 29 (2013) 480–488.
- [8] K. He, L. Dong, Q. Wang, H. Zhang, Y. Li, L. Liu, Z. Zhang, Comparison on the microstructure and corrosion behavior of Inconel 625 cladding deposited by tungsten inert gas and cold metal transfer process, *Surf. Coatings Technol.* 435 (2022) 128245.
- [9] J.I. Ruiz-Vela, J.J. Montes-Rodríguez, E. Rodríguez-Morales, J.A. Toscano-Giles, Effect of cold metal transfer and gas tungsten arc welding processes on the metallurgical and mechanical properties of Inconel® 625 weldings, *Weld. World.* 63 (2019) 459–479.
- [10] M. Karmuhilan, S. Kumanan, Location-dependent microstructure analysis and mechanical behavior of inconel 625 using Cold Metal Transfer (CMT) based wire and arc additive manufacturing, *Vacuum.* 207 (2023) 111682.
- [11] T.A. Rodrigues, V. Duarte, R.M. Miranda, T.G. Santos, J.P. Oliveira, Current Status and Perspectives on Wire and Arc Additive Manufacturing (WAAM), *Materials (Basel)*. 12 (2019).
<https://doi.org/10.3390/ma12071121>.
- [12] M. Cheepu, C.I. Lee, S.M. Cho, Microstructural Characteristics of Wire Arc Additive Manufacturing with Inconel 625 by Super-TIG Welding, *Trans. Indian Inst. Met.* 73 (2020) 1475–1479.
<https://doi.org/10.1007/s12666-020-01915-x>.
- [13] J. Joseph, P. Hodgson, T. Jarvis, X. Wu, N. Stanford, D.M. Fabijanic, Effect of hot isostatic pressing on the microstructure and mechanical properties of additive manufactured AlxCoCrFeNi high entropy alloys,

Mater. Sci. Eng. A. 733 (2018) 59–70.

<https://doi.org/https://doi.org/10.1016/j.msea.2018.07.036>.

- [14] Q. Jiang, P. Zhang, Z. Yu, H. Shi, S. Li, D. Wu, H. Yan, X. Ye, J. Chen, Microstructure and Mechanical Properties of Thick-Walled Inconel 625 Alloy Manufactured by Wire Arc Additive Manufacture with Different Torch Paths, *Adv. Eng. Mater.* 23 (2021) 2000728. <https://doi.org/https://doi.org/10.1002/adem.202000728>.
- [15] S. Selvi, A. Vishvaksenan, E. Rajasekar, Cold metal transfer (CMT) technology-An overview, *Def. Technol.* 14 (2018) 28–44.
- [16] C.G. Pickin, S.W. Williams, M. Lunt, Characterisation of the cold metal transfer (CMT) process and its application for low dilution cladding, *J. Mater. Process. Technol.* 211 (2011) 496–502.
- [17] V. Votruba, I. Diviš, L. Pilsová, P. Zeman, L. Beránek, J. Horváth, J. Smolík, Experimental investigation of CMT discontinuous wire arc additive manufacturing of Inconel 625, *Int. J. Adv. Manuf. Technol.* 122 (2022) 711–727. <https://doi.org/10.1007/s00170-022-09878-7>.
- [18] A. Zavdoveev, V. Pozniakov, T. Baudin, H.S. Kim, I. Klochkov, S. Motrunich, M. Heaton, P. Aquier, M. Rogante, A. Denisenko, A. Gajvoronskiy, M. Skoryk, Optimization of the pulsed arc welding parameters for wire arc additive manufacturing in austenitic steel applications, *Int. J. Adv. Manuf. Technol.* 119 (2022) 5175–5193. <https://doi.org/10.1007/s00170-022-08704-4>.
- [19] C. Zhang, Z. Qiu, H. Zhu, Z. Wang, O. Muránsky, M. Ionescu, Z. Pan, J. Xi, H. Li, On the effect of heat input and interpass temperature on the performance of inconel 625 alloy deposited using wire arc additive manufacturing–cold metal transfer process, *Metals (Basel)*. 12 (2022) 46.